Debris streams in the solar neighbourhood as relicts from the formation of the Milky Way

Amina Helmi*, Simon D. M. White†, P. Tim de Zeeuw*
& HongSheng Zhao*

* *Leiden Observatory, PO Box 9513, 2300 RA Leiden, The Netherlands*
† *Max-Planck-Institut für Astrophysik, Karl-Schwarzschild-Strasse 1,
85740 Garching bei München, Germany*

It is now generally believed that galaxies were built up through gravitational amplification of primordial fluctuations and the subsequent merging of smaller precursor structures. The stars of the structures that assembled to form the Milky Way should make up much or all of its bulge and halo, in which case one hopes to find 'fossil' evidence for those precursor structures in the present distribution of halo stars. Confirmation that this process is continuing came with the discovery of the Saggittarius dwarf galaxy[1], which is being disrupted by the Milky Way, but direct evidence that this process provided the bulk of the Milky Way's population of old stars has hitherto been lacking. Here we show that about ten per cent of the metal-poor stars in the halo of the Milky Way, outside the radius of the Sun's orbit, come from a single coherent structure that was disrupted during or soon after the Galaxy's formation. This object had a highly inclined orbit about the Milky Way at a maximum distance of ~16 kpc, and it probably resembled the Fornax and Sagittarius dwarf spheroidal galaxies.

Early studies treated the formation of the Milky Way's spheroid as an isolated collapse, argued to have been either rapid and 'monolithic'[2], or inhomogeneous and slow compared to the motions of typical halo stars[3]. A second dichotomy distinguished 'dissipationless' galaxy formation, in which stars formed before collapse[4], from 'dissipative' models in which the collapsing material was mainly gaseous[5]. Aspects of these dichotomies remain as significant issues in current theories[6], but they are typically rephrased as questions about whether small units equilibrate and form stars before they are incorporated into larger systems, and about whether they are completely disrupted after such incorporation. Stars from Galactic precursors should be visible today either as 'satellite' galaxies, if disruption was inefficient, or as part of the stellar halo and bulge, if it was complete.

Recent work[7] examined the present-day distribution expected for the debris of a precursor which was disrupted during or soon after the formation of the Milky Way. Objects which could contribute substantially to the stellar halo near the Sun must have had relatively short orbital periods. Ten Gyr after disruption their stars should be spread evenly through a large volume, showing none of the trails characteristic of currently disrupting systems like Sagittarius[8]. In any relatively small region, such as the solar neighbourhood, the stars should be concentrated into a number of coherent 'streams' in velocity space, each showing an internal-velocity dispersion of only a few km s^{-1}. Objects initially similar to the Fornax or Sagittarius dwarf galaxies should give rise to a few streams in the vicinity of the Sun.

The high-quality proper motions provided by the Hipparcos satellite allow us to construct accurate three-dimensional velocity distributions for almost-complete samples of nearby halo stars. On the basis of two recent observational studies[9,10], we define a sample containing 97 metal-deficient ([Fe/H] $\leq$ −1.6 dex) red giants and RR Lyrae stars within 1 kpc of the Sun and with the following properties: (1) Hipparcos proper motions are available for 88 of them[11]; for the remaining stars there are ground-based

measurements[12]; in all cases accuracies of a few mas yr^{-1} are achieved. (2) Radial velocities have been measured from the ground, with accuracies of the order of 10 km s^{-1}. Metal abundances have been determined either spectroscopically or from suitable photometric calibrations[13–15]. (3) Calibrations of absolute magnitude M_V against [Fe/H], for red giants[13–15] and RR Lyrae[16] stars, allow photometric parallaxes to be derived to an accuracy of roughly 20%. These are more accurate than the corresponding Hipparcos trigonometric parallaxes, but still remain the largest source of uncertainty in the derived tangential velocities. (4) We estimate the completeness to be of the order of ~92%, based on the fact that there are eight known giants which satisfy our selection criteria but do not have measured proper motions.

We look for substructure in our set of halo stars by studying the entropy S of the sample, defined as:

$$S = -\sum_i \frac{N_i}{N} \log \frac{N_i A_\mathrm{P}}{N} \qquad (1)$$

where the sum is over the A_P elements of the partition, the ith element contains N_i stars, and N is the total number of stars. In the presence of substructure the measured entropy will be smaller than that of a smooth distribution, and will depend on the details of the partition; some partitions will enhance the signal, whereas others will smear it out. If there is no substructure then all partitions will yield similar S values, and no significant minimum value will be found.

We implement this entropy test initially by partitioning velocity space into cubic cells 70 km s^{-1} on a side. This choice is a compromise. It leaves a large number of cells in the high-velocity range empty, but in the regions containing most of the stars, there are at least a few stars per cell.

It is necessary to quantify the significance of any observed low entropy value relative to the distribution expected in the absence of substructure. Here we do this by generating Monte Carlo realizations which test whether the kinematics of the sample are consistent with a multivariate gaussian distribution[17]. We calculate entropies for 10,000 Monte Carlo samples on the same partition as the real
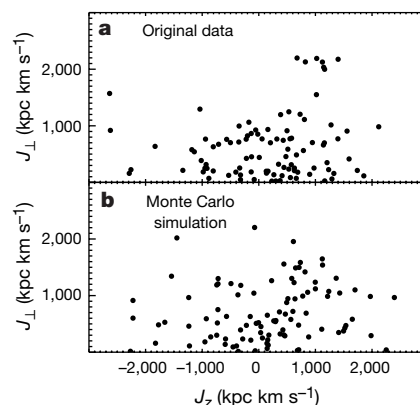

Figure 1 The distribution of nearby halo stars in the plane of angular momentum components, J_z versus $J_\perp = \sqrt{J_x^2 + J_y^2}$. Data are shown for our near-complete sample (**a**) and for one Monte Carlo realization (**b**). Our Monte Carlo data sets have the same number of stars and the same spatial distribution as the observed sample. The characteristics parameters of the multivariate gaussian used to describe the kinematics are obtained by fitting to the observed mean values and variances after appropriate convolution with the observational errors. We then generate 10,000 'observed' samples as follows. A velocity is drawn from the underlying multivariate gaussian; it is transformed to a proper motion and radial velocity (assuming the observed parallax and position on the sky); observational 'errors' are added to the parallax, the radial velocity and the proper motion; these 'observed' quantities are then transformed back to an 'observed' velocity. Velocities are referred to the Galactic Centre; we adopt 8 kpc as the distance to the Galactic Centre and 220 km s^{-1} towards galactic longitude $l = 0$ and galactic latitude $b = 0$ as the velocity of the local standard of rest.

data; only for 5.6% do we find values of S smaller than observed. We have repeated this test for many partitions, finding a large number with probabilities as low or lower than this. In particular, for a partition with a 250 km s^{-1} bin in v_ϕ, and 25 km s^{-1} bins in v_R and v_z, (v_R, v_ϕ and v_z are the velocity components in the radial, azimuthal and z-directions respectively), only 0.06% of Monte Carlo simulations have S smaller than observed. In general, cubic cells yield lower significance levels, suggesting that the detected structure may be elongated along v_ϕ. We conclude that a multivariate gaussian does not properly describe the distribution of halo star velocities in the solar neighbourhood.

At this point the main problem is to identify the structure which makes the observed data incompatible with a smooth velocity distribution. A comparison of the three principal projections of the observed distribution to similar plots for our Monte Carlo samples reveals no obvious differences. To better identify streams we turn to the space of adiabatic invariants. Here clumping should be stronger, as all stars originating from the same progenitor have very similar integrals of motion, resulting in a superposition of the corresponding streams. We focus on the plane defined by two components of the angular momentum: J_z and $J_\perp = \sqrt{J_x^2 + J_y^2}$, although $J_\perp$ is not fully conserved in an axisymmetric potential. In Fig. 1a we plot J_z versus $J_\perp$ for our sample. For comparison, Fig. 1b gives a similar plot for one of our Monte Carlo samples. For $J_\perp \lesssim 1{,}000$ kpc km s^{-1} and $|J_z| \lesssim 1{,}000$ kpc km s^{-1}, the observed distribution appears fairly smooth. In this region we find stars with relatively low angular momentum and at all inclinations. In contrast, for $J_\perp \gtrsim 1{,}000$ kpc km s^{-1}, there are a few stars moving on retrograde low-inclination orbits, an absence of stars on polar orbits, and an apparent 'clump' on a prograde high-inclination orbit.

To determine the significance of this clumping, and to confirm it as the source of the signal detected by our entropy test, we compare the observed star counts in this plane to those for our Monte Carlo data sets. We count how many stars fall in each cell of a given partition of this angular momentum plane and compare it to the expected number in the Monte Carlo simulations. We say that the ith cell has a significant overdensity if there is less than 1% probability of obtaining a count as large as the observed N^i from a Poisson distribution with mean $\langle N^i \rangle = N_{\text{sim}}^{-1} \sum_{j=1}^{N_{\text{sim}}} N_j^i$, where N_j^i is the count in the ith cell of the jth simulation, and N_{sim} is the number of simulations. We repeat this test for a series of regular partitions of $p \times q$ elements, with p, q ranging from 3 to 20, thus allowing a clear

identification of the deviant regions. We find a very significant deviation in most partitions for cells with $J_\perp \approx 2{,}000$ kpc km s^{-1} and $500 < J_z < 1{,}500$ kpc km s^{-1}; the probabilities of the observed occupation numbers range from 0.03% to 0.98%, depending on the partition, and in some partitions more than one cell is significantly overdense.

Given this apparently significant evidence for substructure in the local halo, we investigate what happens if we relax our metallicity and distance selection criteria. We proceed by including in our sample all red giants and RR Lyrae stars studied by Chiba and Yoshii[10] with metallicities less than −1 dex and distances to the Sun of less than 2.5 kpc. This new sample contains 275 giant stars and adds 5 new stars to the most significant clump in our complete sample. Of the 13 members of the clump, 9 have [Fe/H] ≤ − 1.6, whereas the remaining 4 have $\langle$[Fe/H]$\rangle \approx - 1.53 \pm 0.12$, indicating that they are also very metal-poor. These stars are distributed all over the sky with no obvious spatial structure.

In Fig. 2 we highlight the kinematic structure of the clump in the extended sample. The clump stars are distributed in two streams moving in opposite directions perpendicular to the Galactic plane, with one possible outlier. This star has $v_R = 285 \pm 21$ km s^{-1}, and we exclude it because its energy is too large to be consistent with the energies of the other members of the clump. The velocity dispersions for the stream with negative v_z (9 stars) are $\sigma_\phi = 30 \pm 17$, $\sigma_R = 105 \pm 16$ and $\sigma_z = 24 \pm 28$ in km s^{-1}, whereas for the stream with positive v_z (3 stars) these are $\sigma_\phi = 49 \pm 22$, $\sigma_R = 13 \pm 33$ and $\sigma_z = 31 \pm 28$ in km s^{-1}. An elongation in the v_R direction is expected for streams close to their orbital pericentre (the closest distance to the Galactic Centre; compare with other plots of simulated streams[7]).

The orbit of the progenitor system is constrained by the observed positions and velocities of the stars. The orbital radii at apocentre and pericentre are $r_{\text{apo}} \approx 16$ kpc and $r_{\text{peri}} \approx 7$ kpc, the maximum height above the plane is $z_{\text{max}} \approx 13$ kpc, and the radial period is $P \approx 0.4$ Gyr, for a Galactic potential including a disk, bulge and dark halo[8]. We run numerical simulations of satellite disruption in this potential to estimate the initial properties of the progenitor. After 10 Gyr of evolution, we find that the observed properties of the streams detected can be matched by stellar systems similar to dwarf spheroidals with initial velocity dispersions σ in the range 12–18 km s^{-1} and core radii R of 0.5–0.65 kpc. We also analysed whether the inclusion of an extended dark halo around the initial object would affect the structures observed and found very little effect. We
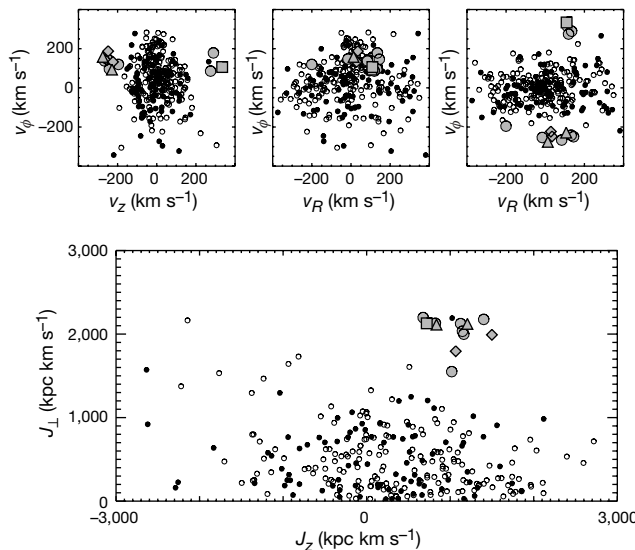

Figure 2 The distribution of nearby halo stars in velocity space and in the J_z–$J_\perp$ plane. Data are shown for our original sample (filled circles) and for the extended sample of more metal-rich and more distant giants[10] (open circles). Candidates for our detected substructure are highlighted in grey: triangles indicate more metal-rich giant stars at distances >1 kpc, diamonds indicate more metal-rich giants at ≤1 kpc, squares indicate metal-poor giants at >1 kpc, and circles indicate metal-poor giants at ≤1 kpc.

derive the initial luminosity L from $L = L^*/(f^{giant} C^* f^{sim})$, where $L^* = 350 L_\odot$ is the total luminosity of the giants in the clump in our near-complete sample, $f^{giant} \approx 0.13$ is the ratio of the luminosity in giants with M_V and $(B-V)$ in the range observed to the total luminosity of the system for an old metal-poor stellar population[18], $C^* = 0.92$ is our estimated completeness, and $f^{sim} \approx 1.9 \times 10^{-4}$ is the fraction of the initial satellite contained in a sphere of 1 kpc radius around the Sun as determined from our simulations. This gives $L \approx 1.5 \times 10^7 L_\odot$, from which we can derive, using our previous estimates of the initial velocity dispersion and core radii, an average initial core mass-to-light ratio $M/L \approx 3$–$10 \Upsilon_\odot$, where $\Upsilon_\odot$ is the mass-to-light ratio of the Sun. A progenitor system with these characteristics would be similar to Fornax. Moreover, the mean metal abundance of the stars is consistent with the derived luminosity, if the progenitor follows the known metallicity–luminosity relation of dwarf satellites in the Local Group[19].

The precursor object was apparently on an eccentric orbit with a relatively large apocentre. Given that it contributes 7/97 of the local halo population, our simulations suggest that it should account for 12% of all metal-poor halo stars outside the solar circle. Figure 2 shows that there are few other halo stars on high angular-momentum polar orbits in the solar neighbourhood, just the opposite of the observed kinematics of satellites of the Milky Way[20]. The absence of satellite galaxies on eccentric non-polar orbits argues that some dynamical process preferentially destroys such systems; their stars should then end up populating the stellar halo. As we have shown, the halo does indeed contain fossil streams with properties consistent with such disruption. □

1. Ibata, R., Gilmore, G. & Irwin, M. J. A dwarf satellite galaxy in Sagittarius. *Nature* **370**, 194–196 (1994).
2. Eggen, O. J., Lynden-Bell, D. & Sandage, A. R. Evidence from the motions of old stars that the Galaxy collapsed. *Astrophys. J.* **136**, 748–766 (1962).
3. Searle, L. & Zinn, R. Compositions of halo clusters and the formation of the galactic halo. *Astrophys. J.* **225**, 357–379 (1978).
4. Gott, J. R. Recent theories of galaxy formation. *Annu. Rev. Astron. Astrophys.* **15**, 235–266 (1977).
5. Larson, R. B. Models for the formation of elliptical galaxies. *Mon. Not. R. Astron. Soc.* **173**, 671–699 (1975).
6. White, S. D. M. & Frenk, C. S. Galaxy formation through hierarchical clustering. *Astrophys. J.* **379**, 52–79 (1991).
7. Helmi, A. & White, S. D. M. Building up the stellar halo of the Galaxy. *Mon. Not. R. Astron. Soc.* **307**, 495–517 (1999).
8. Johnston, K. V., Hernquist, L. & Bolte, M. Fossil signatures of ancient accretion events in the Halo. *Astrophys. J.* **465**, 278–287 (1996).
9. Beers, T. C. & Sommer-Larsen, J. Kinematics of metal-poor stars in the Galaxy. *Astrophys. J. Suppl. Ser.* **96**, 175–221 (1995).
10. Chiba, M. & Yoshii, Y. Early evolution of the Galactic halo revealed from Hipparcos observations of metal-poor stars. *Astron. J.* **115**, 168–192 (1998).
11. *The Hipparcos and Tycho Catalogues* (SP-1200, European Space Agency, ESA Publications Division, ESTEC, Noordwijk, The Netherlands, 1997).
12. Roeser, S. & Bastian, U. A new star catalogue of SAO type. *Astron. Astrophys. (suppl.)* **74**, 449–451 (1988).
13. Anthony-Twarog, B. J. & Twarog, B. A. Reddening estimation for halo red giants using uvby photometry. *Astron. J.* **107**, 1577–1590 (1994).
14. Beers, T. C., Preston, G. W., Shectman, S. A. & Kage, J. A. Estimation of stellar metal abundance. I—Calibration of the Ca II K index. *Astron. J.* **100**, 849–883 (1990).
15. Norris, J., Bessell, M. S. & Pickles, A. J. Population studies. I. The Bidelman-MacConnell "weak-metal" stars. *Astrophys. J. Suppl. Ser.* **58**, 463–492 (1985).
16. Layden, A. C. The metallicities and kinematics of RR Lyrae variables 1: New observations of local stars. *Astron. J.* **108**, 1016–1041 (1994).
17. Sommer-Larsen, J., Beers, T. C., Flynn, C., Wilhelm, R. & Christensen, P. R. A dynamical and kinematical model of the Galactic stellar halo and possible implications for Galaxy formation scenarios. *Astrophys. J.* **481**, 775–781 (1997).
18. Bergbusch, P. A. & VandenBerg, D. A. Oxygen-enhanced models for globular cluster stars. II. Isochrones and luminosity functions. *Astrophys. J. Suppl. Ser.* **18**, 163–220 (1992).
19. Mateo, M. Dwarf galaxies of the Local Group. *Annu. Rev. Astron. Astrophys.* **36**, 435–506 (1998).
20. Lynden-Bell, D. & Lynden-Bell, R. M. Ghostly streams from the formation of the Galaxy's halo. *Mon. Not. R. Astron. Soc.* **275**, 429–442 (1995).

Acknowledgements

Multiple stellar populations in the globular cluster ω Centauri as tracers of a merger event

Y.-W. Lee*, J.-M. Joo*, Y.-J. Sohn*, S.-C. Rey*, H.-c. Lee* & A. R. Walker†

* *Center for Space Astrophysics, Yonsei University, Seoul 120-749, Korea*
† *National Optical Astronomy Observatories/Cerro Tololo Interamerican Observatory (NOAO/CTIO), Casilla 603, La Serena, Chile*

The discovery of the Sagittarius dwarf galaxy[1], which is being tidally disrupted by and merging with the Milky Way, supports the view that the halo of the Galaxy has been built up at least partially by the accretion of similar dwarf systems. The Sagittarius dwarf contains several distinct populations of stars[2,3], and includes M54 as its nucleus, which is the second most massive globular cluster associated with the Milky Way. The most massive globular cluster is ω Centauri, and here we report that ω Centauri also has several distinct stellar populations, as traced by red-giant-branch stars. The most metal-rich red-giant-branch stars are about 2 Gyr younger than the dominant metal-poor component, indicating that ω Centauri was enriched over this timescale. The presence of more than one epoch of star formation in a globular cluster is quite surprising, and suggests that ω Centauri was once part of a more massive system that merged with the Milky Way, as the Sagittarius dwarf galaxy is in the process of doing now. Mergers probably were much more frequent in the early history of the Galaxy and ω Centauri appears to be a relict of this era.

As part of our investigation of the luminosity–metallicity relation of the RR Lyrae stars in the globular cluster ω Cen, we have obtained 2K BV CCD (charge-coupled device) frames with the CTIO 0.9-m
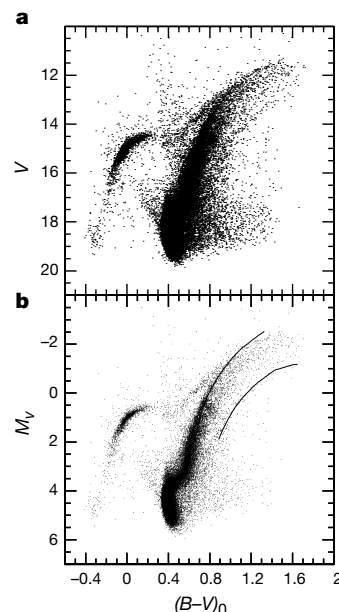

Figure 1 Colour–magnitude diagram of 50,129 stars in the direction of ω Cen. These diagrams were obtained from a mosaic of nine 2K CCD (charge-coupled device) fields. Only stars with at least 20 detections and small photometric errors ($\sigma_V < 0.05$ mag and $\sigma_{B-V} < 0.071$ mag) have been plotted. **a**, All stars in our programme field; **b**, stars located between 2.58 and 15.48 arcmin from the cluster centre. There are several distinct RGBs and a red clump associated with the most metal-rich component. Two RGB loci from the new Yale isochrones[6] (metallicity $Z = 0.0004$, 0.005) are also compared (**b**, solid lines) that bracket the metallicity range of ω Cen. M_V, absolute visual magnitude.